J. Eng. Technol. Sci., Vol. 54, No. 4, 2022, 220406

Geothermal System in Parang Wedang, Yogyakarta, Indonesia

Mochamad Iqbal[1,2,*] & Bella Restu Juliarka[1]

[1]Petrology, Volcanology, and Geothermal Research Group, Geological Engineering, Institut Teknologi Sumatera, Jalan Terusan Ryacudu, Way Huwi, 36365, Lampung, Indonesia.
[2]Graduate School of Engineering, Kyoto University, C1-2-215, Kyoto Daigaku Katsura, Kyoto, 615-8540, Japan.
*E-mail: mochamad.iqbal@gl.itera.ac.id

Highlights:

- Investigation of geothermal system in Parang Wedang, Yogyakarta.
- Subsurface modeling by using magnetic geophysical data.
- Geochemistry analysis of geothermal manifestations.

Abstract. Geothermal manifestations in Parangtritis, Indonesia, known as Parang Wedang Hot Spring, indicate a geothermal system in the subsurface. This circumstance motivated our research to model the Parang Wedang geothermal system in order to determine its subsurface conditions. Geological mapping, the geophysical method, and geochemical analysis were integrated to produce a conceptual model of the Parang Wedang geothermal system. The study area consists of structural hills, karst hills, and eolian plains with andesite breccias, limestone, andesite, and sand deposits as lithological variations. The results of magnetic modeling indicate that the research area is associated with the presence of an andesite intrusion and shows a NE-SW trending geological structure that is thought to be a path for hydrothermal fluid to the surface. Geochemical analysis was performed at two hot springs with temperatures of 47 °C and 49 °C. Geothermometer calculation showed that the geothermal reservoir in Parang Wedang has a temperature of 100 to 120 °C, a depth of about 180 to 285 m, and can be classified as a low enthalpy geothermal system.

Keywords: *geomagnetic; geothermal system; intrusion-related; low-enthalpy; Parang Wedang.*

1 Introduction

Geothermal resources refer to renewable energy stored in the earth. It is a type of clean energy with many functions and wide applications. In addition to power generation and heating, it is widely used in greenhouses, animal captivity, tourism, and the extraction of chemical raw materials [1]. Indonesia has 324

Received May 9th, 2021, 1st Revision February 3rd, 2022, 2nd Revision March 17th, 2022, Accepted for publication March 24th, 2022.
 ISSN: 2337-5779, DOI: 10.5614/j.eng.technol.sci.2022.54.4.6

potential geothermal locations, with a total potential of 29.51 GWe [2] spread over two geological environments, volcanic and non-volcanic, at around 80% and 20%, respectively. Volcanic-associated geothermal environments are now widely developed and produce electrical energy utilized for power plants [3], in contrast with non-volcanic environments, which have not been developed optimally yet. One of the low-temperature geothermal regions is the Parang Wedang geothermal system.

The Parang Wedang area is located between 8°02'21,21" south latitude and 110°32'88,02" east longitude. Administratively, Parang Wedang is located in Mancingan, Parangtritis, Kretek Sub-district, Bantul District, Yogyakarta Special Region, which is about 30 km from Yogyakarta city, Indonesia. The Parang Wedang area is characterized by two hot springs of 47 °C and 49 °C, respectively. The existence of hot springs is an indicator of the existence of geothermal systems beneath the surface. However, determining the presence of a reservoir and heat source of a geothermal system associated with the hot springs in Parang Wedang is challenging. This geothermal system is a non-volcanic geothermal system associated with Tertiary volcanic activity [4].

Only a few previous studies have been conducted in the Parang Wedang geothermal area. The most detailed and integrated, yet outdated, a study was done by Idral, *et al.* [4]. This paper mentions that the geothermal system in Parang Wedang has a reservoir temperature of around 115 °C (classified as a low-temperature system [5]) and a depth of 600 to 700 m. Also, the study interpreted that seawater contaminated the reservoir fluid, based on the chloride content. Furthermore, their remote sensing study showed that the hot springs in the Parang Wedang area correlate with a relatively high land surface temperature [6]. Stratigraphically, the surrounding area consists of five rock units: Parangkusumo basalt, pyroclastic flow breccia, andesite lava, Wonosari limestone, and Quaternary deposit [7]. These rock units are part of the Nglanggran and Wonosari Formations.

This paper provides an integrated study by using the 3G approach. The first G stands for geological analysis, which was conducted by a detailed survey around the area, including geological mapping, geomorphological, and structural analysis. The second G stands for geochemical analysis of the hot springs to determine the reservoir characteristics. Finally, the third G stands for geophysical modeling to understand the heat source mechanism using the geomagnetic method. The 3G analysis was then integrated into a conceptual 2D model of the geothermal system. However, a magnetotelluric (MT) method could provide better results in subsurface modeling. This is commonly used for geothermal exploration [8,9], but it costs more. Furthermore, the geothermal model was

intended to contribute to geothermal resources in Indonesia, to be utilized either for power plants or local hot springs.

2 Geological Setting

The Parang Wedang area can be found on the Regional Geology Map, Sheet Yogyakarta [10]. According to Bemmelen [9], the physiography of Central-South Central Java (which covers the areas of Mount Merapi, Yogyakarta, Surakarta, and the Southern Mountains) can be divided into two zones, the Solo Zone and the Southern Mountain Zone (Figure 1). The Solo Zone is part of the Central Depression Zone of Java Island. This zone is occupied by the cone of Mount Merapi (±2968 m). The Southeast foot of the volcano is part of the Yogyakarta-Surakarta plain (±100 m to 150 m) composed of alluvium sediment from Mt. Merapi. To the west of the Southern Mountain Zone (Pegunungan Selatan), the plains of Yogyakarta continue up to the southern coast of Java Island, which extends from Parangtritis to the Progo River. The main river flows in the western part are the Progo River and the Opak River, while in the east is the Dengkeng River, a Bengawan Solo tributary.

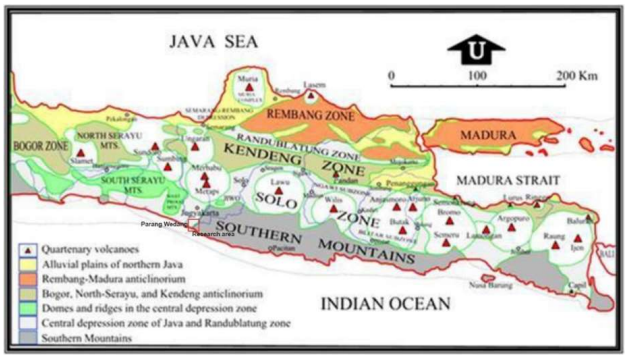

Figure 1 Physiographic map of Java and Madura island [11].

The Southern Mountain Zone is part of the Southern Java Zone [9], whereas tectonically, it is estimated to be located in a basin between volcanic arcs. This zone stretches from Yogyakarta to the east, towards Wonosari, Wonogiri, and Pacitan, and then continues to the southern part of Malang and the Blambangan area. The Southern Mountain Zone can be divided into three subzones, the Northern Subzone, or the Baturagung (Baturagung range), the Central Subzone (the Wonosari Depression), and the Southern Subzone, or the Sewu Mountains (literal meaning: thousand mountains) [11]. Physiographically, the research area covering Parangtritis and its vicinity (including the Parang Wedang area) lies in the Southern Zone of Central Java, which consists of karst mountains from the

Sewu Mountains [12]. The Sewu Mountains subzone has elevations between 0 and 400 meters asl and is composed of limestone and hilly landscapes, with limestone hills forming cones with a height of several tens of meters. This karst landscape stretches from Parangtritis Beach in the west to Pacitan in the east. The Sewu Mountains area is geologically included in the Wonosari Formation, from Central Miocene to Lower Pleistocene in age.

According to Surono in [11], the regional stratigraphy of the Southern Mountain Zone, which covers the Parang Wedang area, consists of the Nglanggran Formation (Tmn), the Wonosari Formation (Tmwl), young volcanic deposits of Merapi Volcano (Qmi), and alluvium (Qa), ordered from old to young. The Nglanggran Formation consists of volcanic breccias, agglomerate, tuff, andesite, and andesite-basalt lava flow with sandstone intercalation, which shows a gravitational deposit marine environment and was deposited during the Early-Middle Miocene. Secondly, the Wonosari Formation forms a well-developed karst morphology composed of reef limestone, bioclastic layers, and calcarenite. These rock units are carbonate depositions from the Middle Miocene to the late Miocene and are well exposed in Wonosari and its surrounding areas. Thirdly, the young volcanic deposits of Merapi Volcano, composed of undifferentiated tuff, ash, breccias, agglomerates, and lava flow, are deposited conformably. Lastly, the most recent deposit of alluvium overlays the formations unconformably.

3 Data and Methods

The research data and methods used in this study are related to three fields, namely geology, geophysics, and geochemistry. Each produced independent conclusions, which were integrated into a geothermal conceptual model. The geothermal model was based on constrained geological conditions, and geomagnetic modeling was based on field observations.

Geological mapping was conducted in the Parang Wedang area, including geomorphological, stratigraphy, petrography, and geological structure observation. First, a geomorphological analysis was carried out by observing contours on topographic maps, confirmed by direct observation in the field. Then, detailed geological maps were made using standard procedures for making geological maps, namely observations and descriptions of outcrops in the field, sampling, analysis of fossils and thin sections (petrography), and measurements of geological structures in the field.

The magnetic rock value was measured using a Proton Precision Magnetometer (PPM) tool, owned by the Geophysics Department of Universitas Gadjah Mada, to help observe variations in the magnetic susceptibility value of rocks below the

surface. Data acquisition was carried out at twenty locations, with a distance of about 200 m between each point, forming a straight line. Firstly, the raw magnetic data were corrected according to the International Geomagnetic Reference Field (IGRF), yielding the total magnetic field anomaly [14-16]. This was used to obtain a reduction to the pole and upward continuation anomaly map. Furthermore, the subsurface modeling was based on upward continuation from 100 m, carried out using the Oasis Montaj software with a trial-and-error approach. A simplification of the geophysical workflow is shown in Figure 2.

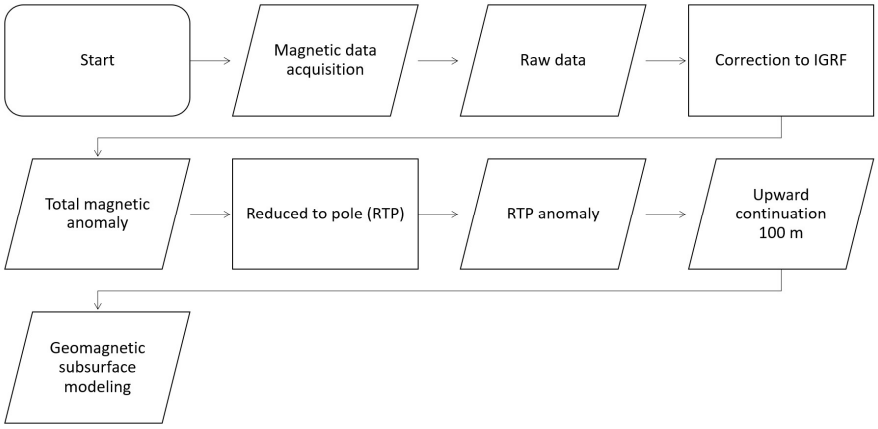

Figure 2 Workflow from geophysical data acquisition to modeling.

Geochemical sampling was performed on two manifestations of warm springs in the Parang Wedang area to determine the major ion content. In addition, sampling was also conducted on groundwater around Parang Wedang and seawater located close to the hot springs to observe the local hydrogeological conditions. The sampling method referred to standard procedures based on Arnórsson (2006) [17] and Nicholson (1993) [20]. The samples were then analyzed at the Yogyakarta BPPTKG Laboratory. The elements analyzed were Li^{+}, Na^{+}, K^{+}, Ca^{2+}, Mg^{2+}, SiO_2, B, Cl^{-}, F^{-}, SO_4^{2-}, HCO_3^{-}, Fe, and Mn, which were used to interpret the conditions of the geothermal reservoir below the surface.

4 Result and Discussion

4.1 Geology

Based on field observation, the research area was divided into three geomorphological units based on morphometry and morphogenesis, namely, the Eolian Plain Unit, the Karst Hills Unit, and the Structural Hills Unit (Figure 3).

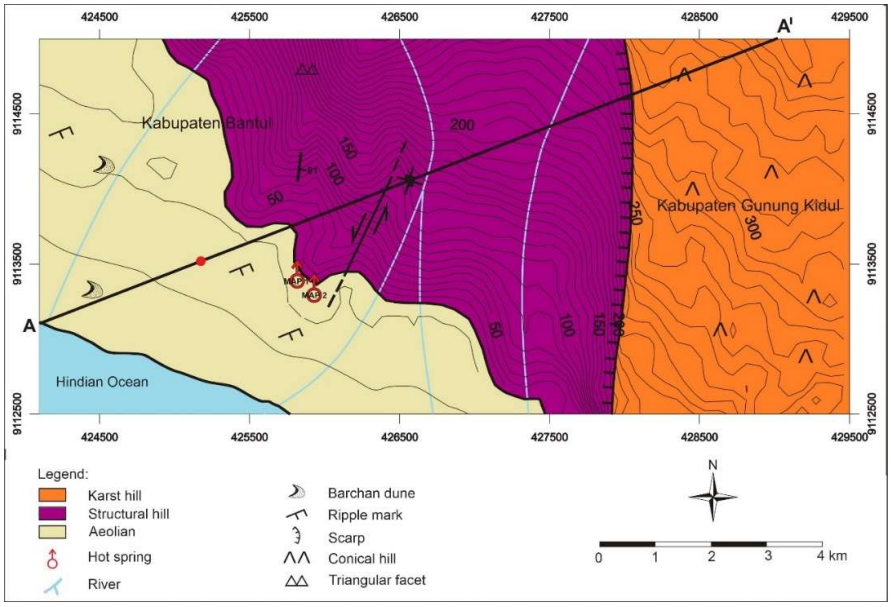

Figure 3 Geomorphological map of the study area.

The Eolian Plain Unit is composed of coarse to fine loose sand with a brown color. The highest elevation is 25 meters and the lowest elevation is 5 meters. This unit is formed from sediment transported from Indian Ocean waves and sediment from the wind blowing. Several barchan dunes form the geomorphology of the eolian plain (Figure 4). The hot springs are discharged in this unit.

Figure 4 A typical barchan dune in the Parang Wedang area. Note that the wind causes an asymmetrical shape. The wind's direction is from the gentle slope to the steeper slope.

Karst hills are located from the eastern to the southern parts of the study area and are the most extensive geomorphological unit in the study area. These karst hills are composed of limestone with a morphology of conical hills with a slope of up to 65° (Figure 5).

Figure 5 Karst hills.

The Structural Hill Unit can be seen from the appearance of a tight contour pattern. This pattern can be described as the morphology of steep hilly areas. The river valleys, generally V-shaped, show a predominance of vertical erosion processes. The morphological features found in the Structural Hill Unit are triangular facets and fault scarps. The triangular facets are one of the features of the structural landscape process. The existence of fault scarps can be evidence of the geological structure appearing on the surface, relatively trending N-S (see Figure 3).

The stratigraphy of Parangtritis and its surrounding areas is composed of Tertiary rocks consisting of an andesite lava unit and a breccia andesite Nglanggran unit, a reef limestone unit, a younger andesite intrusion of Quaternary age, and recent sand deposits. Likewise, a dextral strike-slip fault trending NE-SW also emerges in the andesite lava unit, which could be a permeable pathway for geothermal fluid to reach the surface. A geologic map of the research area is shown in Figure 6.

Petrographic observations of andesite lava in the Parang Wedang geothermal area revealed a porphyro-aphanitic texture with 0.3 alteration intensity (Figure 6). Phenocryst consists of 20% pyroxene and plagioclase with 0.5 to 0.1 mm mineral size. The groundmass is possibly plagioclase microlite, pyroxene, and volcanic glass. Calcite is present at around 10% as a replacement mineral, replacing

plagioclase with a brownish-yellow color. Figure 7 shows thin section of lava andesite from Parang Wedang

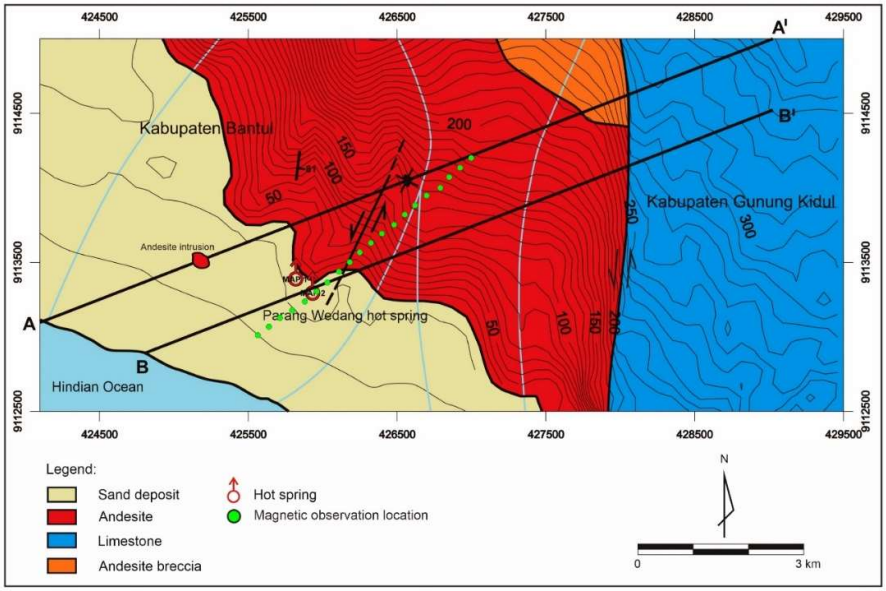

Figure 6 Geologic map of the research area.

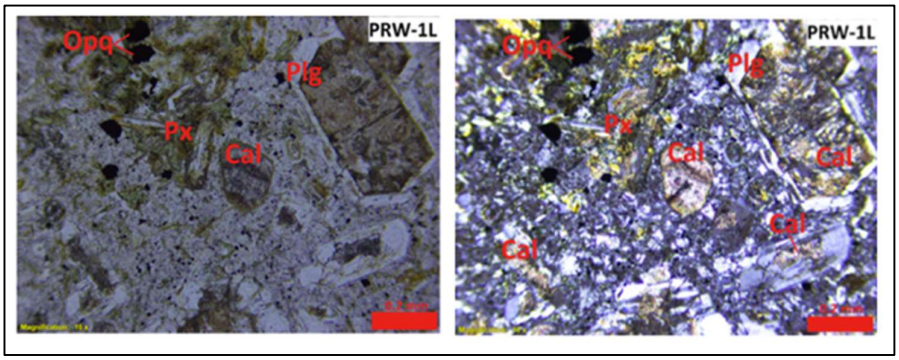

Figure 7 Thin section of lava andesite from Parang Wedang.

The thin section of limestone in the study area shows a mud-supported texture with more than 10% grains. Based on Dunham's classification in [17], the limestone is classified as wackestone. The limestone consists of a 10% large foram (lf) *Flosculinella bontangensis* fossil (Figure 8), which shows a middle Miocene age, equivalent to the Wonosari Formation. This fossil has a yellowish-

gray color, an ovalish shape, and a perforated radial wall structure with a large number of chambers. Furthermore, chlorite (ch) and mica (mc) were found in the thin section, as alteration minerals replacing calcite (ca).

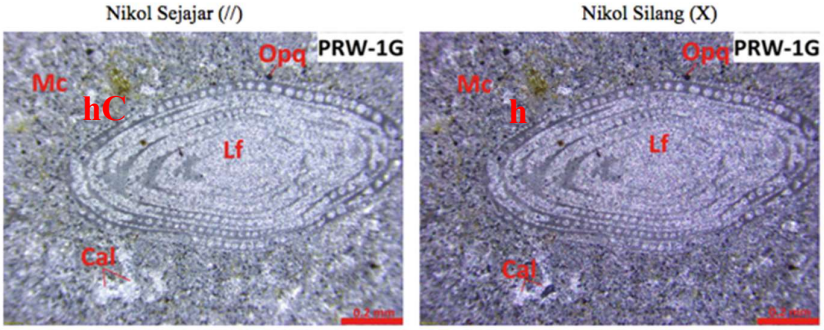

Figure 8 A thin section of the limestone unit shows a *Flosculinella bontangensis* fossil.

4.2 Geomagnetic

4.2.1 Total Magnetic Anomaly

Total magnetic field anomalies were generated by making several corrections to the field's measurement data, namely corrections to the IGRF. Then a magnetic anomaly map was created using the Oasis Montaj GmSys software. The resulting anomaly map was also the result of automatic extrapolation from the Oasis Montaj GmSys software. The topography's contour pattern of the total magnetic field anomaly consisted of many positive and negative closure pairs. These pairs of positive and negative closures indicate a magnetic dipole anomaly. The number of magnetic dipole pairs that show a large amount of total magnetic field anomalies in the topography is still very much influenced by local anomalies.

The total magnetic field anomaly distribution ranged from -523 nT to -173 nT. The high anomaly range is due to the various rock lithologies in the research area: andesite lava, andesite breccias, limestone, and sand deposits. The high anomaly values are marked in red, and low anomalous values are marked in blue. It can be seen on the total magnetic field anomaly map that high anomaly values are found in the southwestern part of the study area (Figure 9).

The obtained total magnetic field anomaly is still influenced by the dipole anomaly and mixed between local and regional anomalies. To eliminate the dipole effect, a reduction to the pole should be performed. Reduction to the pole changes the dipole anomaly to a monopole anomaly.

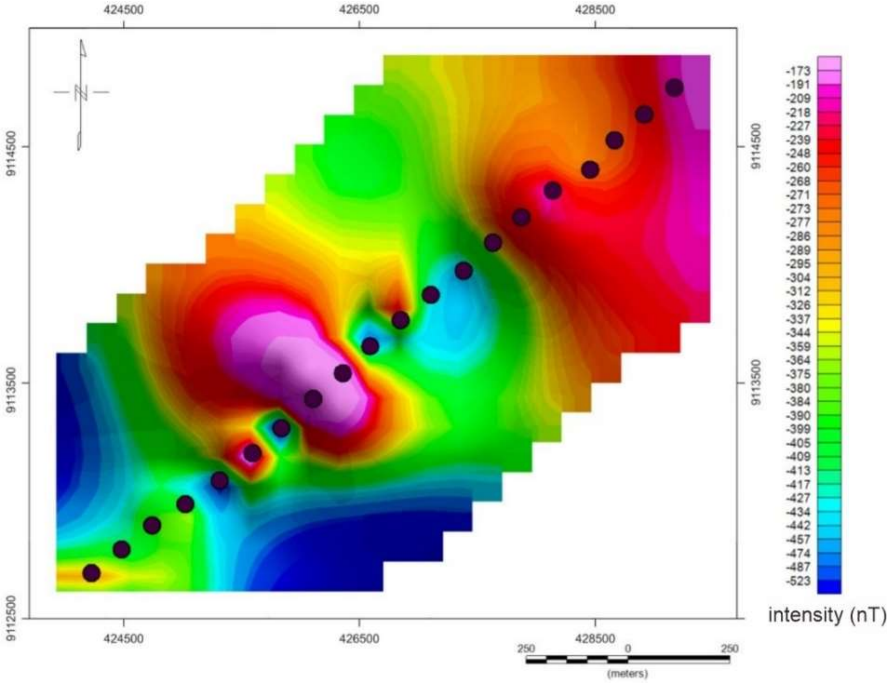

Figure 9 Total magnetic field anomaly in Parang Wedang geothermal area.

4.2.2 Reduction to the Pole (RTP) Magnetic Anomaly

The magnetic field anomaly resulting from reduction to the pole (RTP) is an anomaly that has been reduced to the pole to eliminate the dipole effect from the total magnetic field anomaly. In addition, to make the dipole pattern appear as a monopole, a reduction process to the pole was also carried out, which arranges the anomaly right above the anomaly's cause for easier interpretation.

The RTP value will show that high-value anomalies have high magnetic susceptibility, which can be seen in the northern and southern parts of the study area (Figure 10). The high anomalies in the northern part of the study area have continuity with the NE-SW trend. A low anomaly pattern follows this trend in the middle of the high anomaly. High and low anomaly patterns were identified as subsurface structures. Apart from this pattern, there is a high anomaly in the middle of the study area. This high anomaly pattern probably arises due to lithology differences in the study area, namely between andesite and limestone. Therefore, it is necessary to conduct an upward continuation process to ascertain the research area's estimated structure and lithological boundaries.

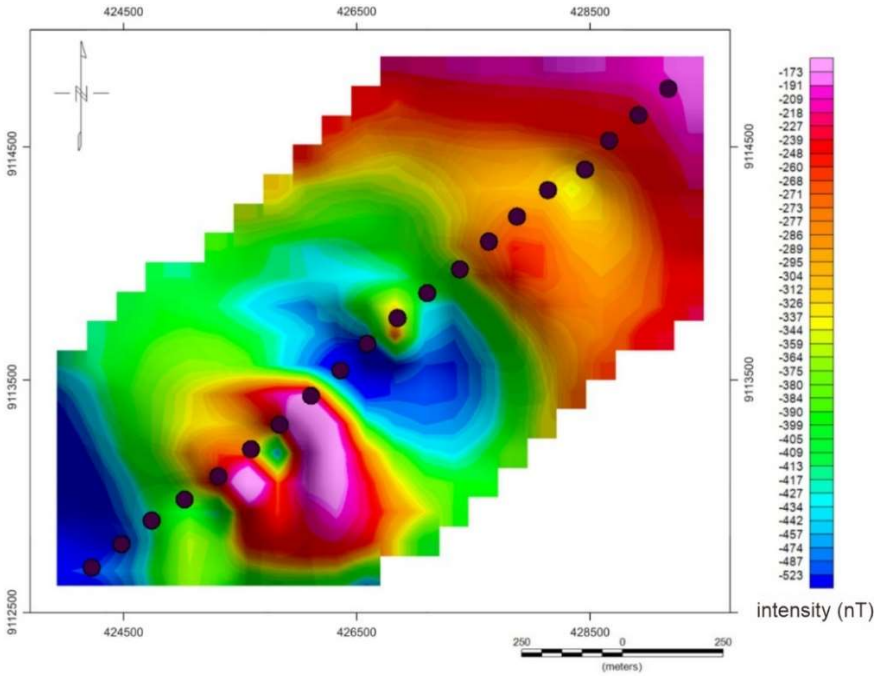

Figure 10 RTP map in Parang Wedang geothermal area.

4.2.3 Upward Continuation Magnetic Anomaly

Upward continuation transformation is a transformation that aims to clarify the anomaly. Another purpose of the upward continuation transformation is to strengthen deep anomalous features and eliminate superficial anomalous features. The difference between the anomaly before and after the upward continuation is the loss of anomalous features with tight contours. The upward continuation process is sufficient if there are no significant changes in the regional anomaly map. The upward continuation value used in this filter was 100 meters because the anomaly is dominant and clearly visible.

On the upward continuation anomaly map of 100 meters, high anomaly values are shown in pink-red, while low anomalies are shown in blue. In Figure 11, there is anomalous contrast, indicated by the presence of side-by-side high and low anomaly values. The adjoining low and high anomaly patterns can be identified as subsurface structures with anomalous contrast boundaries representing the strike direction of the structure. In this study, high anomaly values are > -271 nT, while low anomaly values are < -417 nT. Low magnetic anomalies can indicate reservoirs and heat sources because the rock is hot, decreasing the magnetic

susceptibility value. The magnetic anomaly map shows that a low anomaly is located in the middle and south of the research area. Therefore, low magnetic anomaly values can indicate reservoirs or the heat source of the Parang Wedang geothermal system. We assumed that the heat source is the Ancient Parangtritis volcano in the research area. The results of this upward continuation was then selected to be interpreted by geophysical modeling.

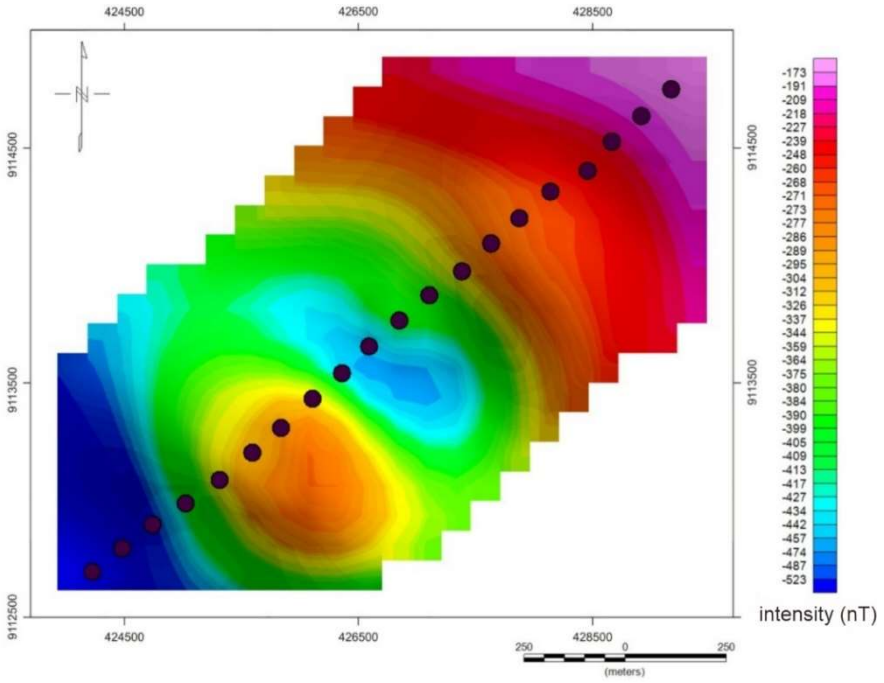

Figure 11 The upward continuation anomaly map upward of 100 m.

4.2.4 2D Geomagnetic Modeling

Magnetic data measurement results are strongly influenced by the anomaly target, daily variation, and regional data. Daily variations were interpolated to magnetic data measurements with time. Regional data were corrected using the IGRF value, referring to WGS 84.

The quantitative interpretation was performed by modeling using the Oasis Montaj GmSys software with continuation upward of 100 m by entering intensity, inclination, and declination. The model should be matched with the observed anomaly. If the anomaly generated from the modeling agrees with the observed anomaly, the position, shape, and model parameters can be assumed and

interpreted as the actual object's position, shape, and parameters. The magnetic modeling is shown in Figure 12.

This modeling process requires additional stratigraphic data and geological maps of the research area. The rock susceptibility value that was used for the modeling is shown in Table 1. The accuracy of the GmSys software for modeling can be seen from the error value; the lower the error rate, the more accurate the modeling. The subsurface modeling was based on a trial-and-error method to pick the smallest error. The best trial-and-error method resulted in an error value of 19.488.

Table 1 Susceptibility value for the subsurface modeling based on Telford *et al.* (1990) [19].

Rock type	Susceptibility (cgs)
Andesite	0.0006
Andesite breccia	0.0005
Andesite intrusion	0.001
Limestone	0.0003
Sand deposit	0.00004

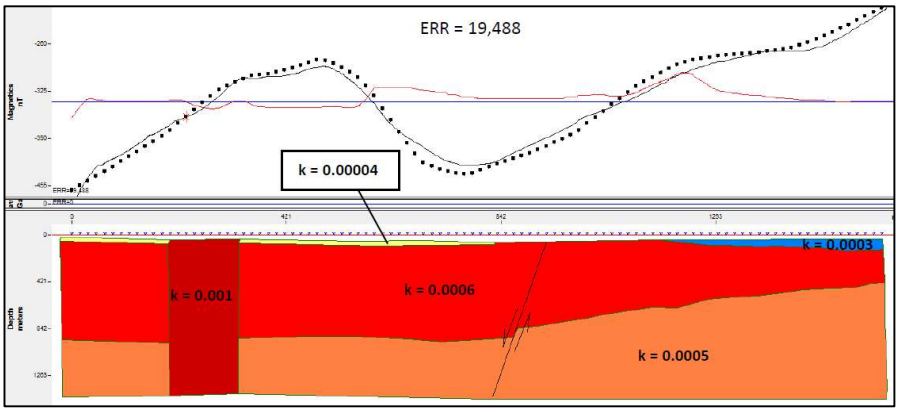

Figure 12 Geomagnetic model of Parang Wedang geothermal area.

Rising and falling geomagnetic anomalies occur on the trajectory, resulting in positive and negative peaks because of the fault identified in the field. The fault or fracture is probably a pathway for geothermal fluid to reach the surface. The geomagnetic modeling results identified a layer deduced as a reservoir, which is located at a depth of approximately 600 meters below the surface and is interpreted as breccia or andesite breccia.

4.3 Geochemistry

There are two warm springs in the research area. Thermal spring 1 (PRW 1) is located in the Parang Wedang hot spring, while the second manifestation (PRW 2) is about 10 m from the first location. PRW 2 is a warm spring caused by a dug well with a 6 m depth. The manifestation characteristics and geochemistry analysis results are presented in Tables 2 and 3. In addition, a geochemistry analysis was also carried out on the groundwater (well) sample taken near a warm spring with 3 m depth and filled with seawater which is located about 300 m to the south of the manifestation.

Table 2 Manifestation and cold water characteristics.

Manifestation	T_{water} (°C)	T_{air} (°C)	pH	Conductivity (umhos/cm)	Explanation
Warm spring 1 (PRW 1)	47 °C	25.6 °C	7.23	13,530	Odorless, discharge cannot be measured, showing bubbles and surrounded by algae.
Warm spring 2 (PRW 2)	49 °C	28.2 °C	7.17	15,873	Clear, odorless, discharge cannot be measured.
Groundwater (SMR)	nm	nm	7.22	1,089	Clear, odorless, 3 m depth.
Seawater (SW)	nm	nm	8.19	45,067	300 m from the manifestation.

Table 3 Geochemistry analysis result of the samples.

Parameters	Warm spring PRW 1	Warm spring PRW 2	Groundwater SMR	Seawater SW
Li^+	0.17	0.19	bdl	0.08
Na^+	1340	1647	75	7825
K^+	23	34	6	434
Ca^{2+}	2107.5	2061.0	102.6	517.5
Mg^{2+}	6.89	11.72	28.35	1233.00
SiO_2	44	42	50	4
B	6	7	bdl	3
Cl^-	5650	6625	81	18088
F^-	2	3	0	1
SO_4^{2-}	488	563	29	2389
HCO_3	85	52	378	141
Fe	bdl	bdl	bdl	0.06
Mn	0.06	0.15	0.02	0.04
Ion balance	2%	6%	9%	8%

bdl: below detection limit.

The thermal springs had a temperature of 47 °C and 49 °C, respectively, with neutral pH and conductivity ranging around 13,530-15,873 umhos/cm. Similarly,

the groundwater showed relatively the same pH with low conductivity (1,089 umhos/cm). However, in contrast with the previous samples, the seawater showed a moderately alkaline pH with very high conductivity of about 45,067 umhos/cm. Therefore, we assume that the geothermal manifestation does not originate from seawater, based on the relatively different conductivity.

The result of the geochemistry analysis was plotted on several ternary diagrams. Plotting on the Cl-SO4-HCO3 diagram showed that both manifestations are chloride-type springs originating from a reservoir (Figure 13). Plotting on the Cl-Li-B ternary diagram showed that the water samples are located in the same plotting, indicating that the manifestations originate from the same reservoir (Figure 14).

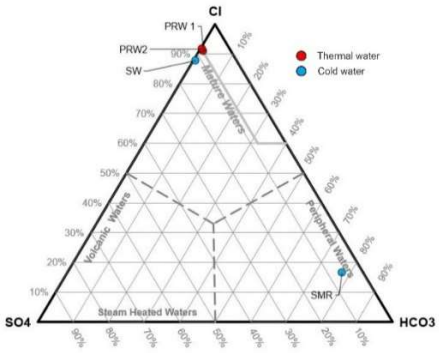

Figure 13 Plotting on Cl-SO4-HCO3 ternary diagram.

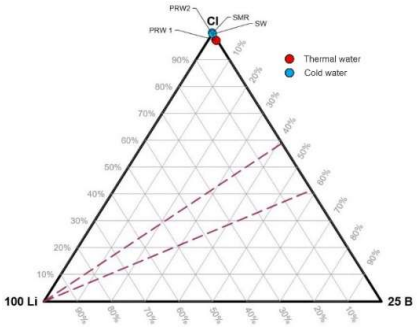

Figure 14 Plotting on the Cl-Li-B ternary diagram.

The ratio between B/Cl in the two manifestations was 0.001. Plotting on the Na-K-Mg diagram (Figure 15) showed that the hot springs are located in a partial equilibrium area with a relatively low Mg value, indicating no mixing with groundwater [20]. However, the contrast value of Mg content between the

manifestation and seawater indicates that the geothermal fluid does not originate from the seawater, which is in line with the conductivity. From the graph, we conclude that the geothermal reservoir in Parang Wedang has a temperature of around 100 to 120 °C, based on Na/K Giggenbach's geothermometer [21]. The depth of the reservoir can be estimated by using statistical data, for which the equation is given by Iqbal *et al.* in [22] as follows:

$$Depth = -0.0257(T^2) + 0.4446T + 31.248 \quad (1)$$

where T = reservoir temperature in °C.

With a reservoir temperature of around 100 to 120 °C, the depth of the reservoir is about 180 to 285 m.

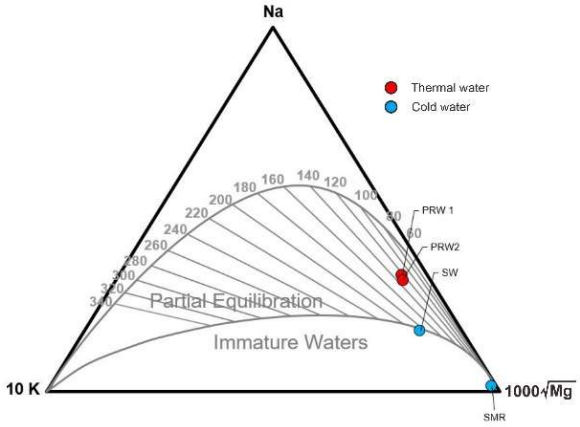

Figure 15 Plotting on the Na-K-Mg ternary diagram.

4.4 Discussion

From the data that was collected and analyzed, a model of the geothermal system in the Parang Wedang area was obtained (Figure 16). Based on the geological mapping, there is an igneous rock intrusion in the study area. This is also supported by Hartono and Bronto (2007) [21], who state that the research area is located in the ancient volcanic area of Parangtritis, which is part of the Nglanggran Formation. From the geomagnetic modeling results, the Parangwedang geothermal system is assumed to have a heat source originating from the andesite intrusion or the ancient Parangtritis volcano, which means the geothermal system is volcanic-related. However, no recently active volcano is found around the area. The closest active volcano is Mt. Merapi, which is quite far, about 40 km to the north, so it is estimated that the geothermal system in Parangwedang is not related to Mt. Merapi's activities. In addition, geochemical

data shows an F content of around 2-3 mg/L in the manifestation, indicating a magmatic influence on the hydrothermal fluid.

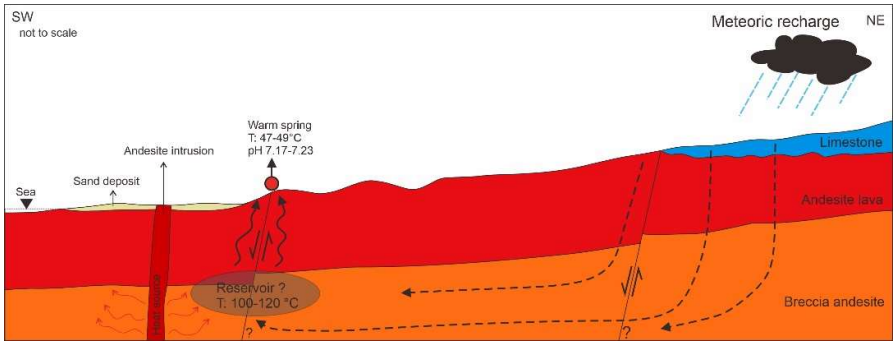

Figure 16 Conceptual model of the Parang Wedang geothermal system.

As the water infiltrates from the recharge area, it moves towards the reservoir, estimated at 100 to 120 °C based on geothermometer calculation, and classified as a low enthalpy/temperature system [20]. The andesite intrusion is interpreted as the heat source, which heats the reservoir conductively. The hydrothermal fluid in the reservoir goes up to the surface through a fault and appears as a warm hot spring with a temperature of around 47 to 49 °C. Low enthalpy is not suitable for generating power. Otherwise, the Parang Wedang geothermal system's utilization that should be emphasized is direct use for local tourism, such as public hot springs [22,23].

5 Conclusion

Physiographically, the research area is located in the Southern Mountains Zone of Java, with the morphology in the study area consisting of structural hills, karst hills, and eolian plains. The geology of the research area consists of andesite breccias, limestone, andesite lava, andesite intrusion, and sand deposits. In addition, two NE-SW trending geological structures were identified in the study area, which is considered to be paths for geothermal manifestations to the surface. From the modeling results, the subsurface profile is dominated by igneous rocks derived from Nglanggran volcanic rock, the Miocene andesitic rocks showing a susceptibility value of 0.0006 cgs. Rock breccias with a susceptibility value of 0.0005 cgs were identified and the andesite intrusion had a susceptibility value of 0.001 cgs. Limestones were identified with a susceptibility value of about 0.0003 cgs. Units of sand deposits (dunes) had a susceptibility value of 0.00004 cgs.

The warm springs that appear on the surface with a temperature of 47 to 49 °C and a neutral pH contain chloride-type water, which is interpreted as water from

a reservoir. Geothermometer calculations determined that the Parang Wedang geothermal reservoir has a temperature of 100 to 120°C and a depth of 180 to 285 m and is related to volcanism originating from the ancient Parangtritis volcano or the andesite intrusion in the study area.

Acknowledgment

The authors express their gratitude to Ibu Pri Utami and Ibu Sintia Windhi Niasari for their guidance and companionship during the research and for being good critics during the writing of this article.

References

[1] Lund, J.W., *Direct Heat Utilization of Geothermal Energy, in Reference Module in Earth Systems and Environmental Sciences*, Elsevier, 2021.

[2] Girianna, M., *Geothermal Handbook for Indonesia*. BAPPENAS, 2014.

[3] Pambudi, N.A., *Geothermal Power Generation in Indonesia, A Country Within the Ring of Fire: Current Status, Future Development and Policy*, Renewable and Sustainable Energy Reviews, **81**, pp. 2893-2901, Jan. 2018.

[4] Idral, A., Suhanto, E., Sumardi, E., Kusnadi, D. & Situmorang, T., *Integrated Geology, Geochemistry and Geophysics Investigation of the Parangtritis Geothermal Area*, Colloquium of Mineral Resources Inventory Results, Bandung, 2003.

[5] Hochstein, M.P. & Browne, P.R.L., *Surface Manifestations of Geothermal Systems with Volcanic Heat Sources*, in Encyclopedia of Volcanoes, 1st ed., Academic Press, 2000.

[6] Tae, Y.D., Florency, F., Putri, R.A., Padjeko, M.A., Senduk, S.E. & Kiswiranti, D., *Identification of Non-Volcanic Geothermal Potential with the Combination of Remote Sensing Data (GIS) and Geological Mapping in Parang Wedang, Kretek District, Bantul Regency*, Special Region of Yogyakarta, 11th Earth Science National Conference, 2018 (Text in Indonesian).

[7] Yudiantoro, D.F., Choiriah, S.U., Paramitahaty, I. & Ardian, M.I.N. *Characteristics and Potential of Geothermal Systems based on Water Geochemistry in Parangtritis Region, Kretek District, Bantul Regency, Special Region of Yogyakarta*, Prosiding LPPM UPN 'VETERAN' Yogyakarta, 2016. (Text in Indonesian)

[8] Singarimbun, A., Gaffar, E.Z. & Tofani, P., *Modeling of Reservoir Structure by Using Magnetotelluric Method in the Area of Mt. Argopuro, East Java, Indonesia*, Journal of Engineering and Technological Sciences, **49**(6), pp. 833-847, Dec. 2017.

[9] Grandis, H., Warsa, W. & Sumintadireja, P., *Layer Stripping in Magnetotellurics (MT) for Enhancement of Resistivity Change Effect in Reservoir: Equivalence Analysis*, Journal of Engineering and Technological Sciences, **52**(2), pp. 258-270, Apr. 2020.
[10] Rahardjo, W., Sukandarrumidi & Rosidi, H., *Geological Map Sheet Yogyakarta, Java Scale 1:100,000*, Geological Agency, 1995 (Text in Indonesian).
[11] van Bemmelen, R.W., *The Geology of Indonesia*, The Hague: Govt. Print. Off, 1949.
[12] Pannekoek, A.J., *Outline of the Geomorpohology of Java*. E.J. Brill, 1949.
[13] Surono, S., *Litostratigraphy of the Eastern Southern Mountains of the Special Region of Yogyakarta and Central Java*, Jurnal Geologi dan Sumberdaya Mineral, **19**(3), pp. 209-221, Jun. 2009, (Text in Indonesian).
[14] Pollack, A., Cladouhos, T.T., Swyer, M.W., Siler, D., Mukerji, T. & R. N. Horne, *Stochastic Inversion of Gravity, Magnetic, Tracer, Lithology, And Fault Data for Geologically Realistic Structural Models: Patua Geothermal Field Case Study*, Geothermics, **95**, 102129, Sep. 2021.
[15] Abdel Zaher, M., Saibi, H., Mansour, K., Khalil, A. & Soliman, M., *Geothermal exploration using airborne gravity and magnetic data at Siwa Oasis, Western Desert, Egypt*, Renewable and Sustainable Energy Reviews, **82**, pp. 3824-3832, Feb. 2018.
[16] Grabowska, T. & Bojdys, G., *Analysis of geomagnetic field along seismic profile P4 of the International Project POLONAISE'97*, Tectonophysics, **383**(1), pp. 15-28, May 2004.
[17] Arnórsson, S., Bjarnason, J.Ö., Giroud, N., Gunnarsson I. & Stefánsson, A., *Sampling and Analysis of Geothermal Fluids*, Geofluids, **6**(3), pp. 203-216, 2006.
[18] Dunham, R.J., *Classification of Carbonate Rocks According to Depositional Textures*, **38**, pp. 108-121, 1962.
[19] Telford, W.M. & Sheriff, R.E., *Applied Geophysics*. Cambridge University Press, 1990.
[20] Nicholson, K., *Geothermal Fluids*. Springer Berlin Heidelberg, 1993.
[21] Giggenbach, W.F., *Geothermal Solute Equilibria, Derivation of Na-K-Mg-Ca geoindicators*, Geochimica et Cosmochimica Acta, **52**(12), pp. 2749-2765, Dec. 1988.
[22] Iqbal, M., Herdianita, N.R. & Risdianto, D., *Characteristic of Geothermal Fluid at East Manggarai, Flores, East Nusa Tenggara*, IOP Conf. Ser.: Earth Environ. Sci., **42**(1), 012016, 2016.
[23] Hartono, G. & Bronto, S., *The Origins of the Formation of Mount Batur in the Wediombo Area, Gunungkidul, Yogyakarta*, Indonesian Journal on Geoscience, **2**(3), Art. no. 3, Sep. 2007 (Text in Indonesian).
[24] Anderson, D.N. & Lund, J., *Direct Utilization of Geothermal Energy: A Technical Handbook*, Jan. 1979.

[25] Saptadji, N.M., *Geothermal Engineering,* 1st ed. ITB Press, 2018. (Text in Indonesian)